

Ag₂O–MnO₂/Graphene Oxide Nanocomposite

Subjects: Chemistry, Inorganic & Nuclear

Contributor: Syed Adil, Mujeeb Khan, Mohammed Rafi Shaik, Mufsir Kuniyil, M Rafiq Siddiqui, Abdulrahman Al-Warthan

Catalytic oxidation of alcohol to their analogous carbonyls is one of the key organic reactions in both scientific and industrial applications, with universal production of 10,000 million tons/year of carbonyls in the 20th century. Such as, aldehyde and ketone derivatives are extensively employed as precursors in insecticide, flame-retardant, cosmetic, confectionery, flavoring, pharmaceutical, and beverage industries.

Keywords: Ag₂O nanoparticles ; graphene oxide ; nanocomposite ; MnO₂ ; oxidation ; catalyst

1. Introduction

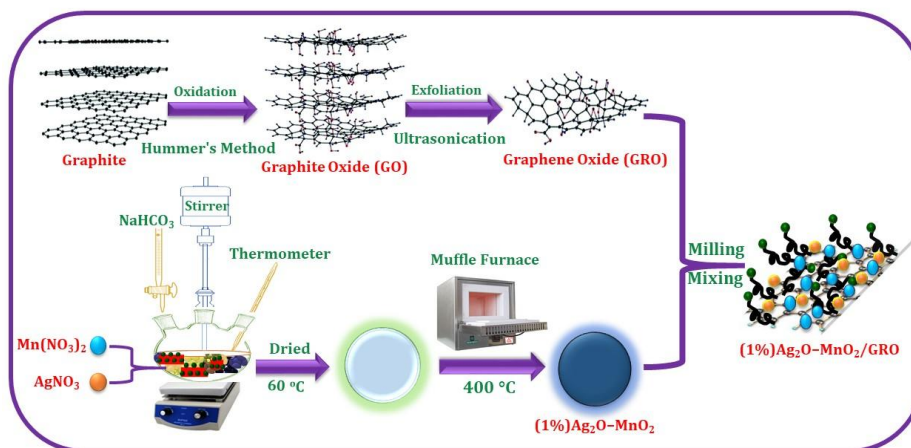
Traditionally, the current oxidation process depends on the utilization of strong stoichiometric oxidizing agents, which are usually expensive and toxic (e.g., permanganate, hypochlorite, or dichromate, etc.) [3]. Moreover, the strong nature of these conventional oxidizing agents leads to an over-oxidation of alcohols to CO₂ or carboxylic acids, thus decreasing the selectivity towards aldehydes [4]. Alternatively, due to the growing environmental concerns, the applications of eco-friendly oxidants, such as molecular O₂ and aqueous H₂O₂, have been preferred, which only produces water as the by-product [5].

Moreover, graphene-based materials have also attracted increasing attention in the field of catalysis due to their extraordinary optical, electronic, and catalytic properties [6]. The unique 2D structure of graphene allows introducing a variety of functionalities on its surface through covalent and non-covalent interactions [7]. This property can be successfully exploited for the development of graphene-based sustainable catalysts [8]. In this regard, the precursors of graphene, i.e., graphene oxide (GRO)-based materials, have generated significant excitement in the field of catalysis due to their remarkable physicochemical and surface properties [9]. Particularly, the presence of a variety of oxygenated groups, a large number of defects, and a unique 2D structure have rendered graphene oxide as perfect material in catalysis [10]. In addition, the negatively charged surface of GRO can be easily exploited for the dispersion of other catalytically active materials, including metal and metal oxide nanoparticles (NPs), on its surface to enhance their resulting properties [11][12]. Several metal and/or metal oxide NPs like Pd [13], Ag [14], Co₃O₄ [15], ZrO₂ [16], and Fe₂O₃ [17] have incorporated on GRO nanolayers and achieved superior performance and selectivity. Recently, GRO-based metal nanocomposites have been explored and exhibited considerable potential in the oxidation of various organic moieties, including alcohols [18], cyclohexane [19], amines [20], benzene [21], aryl benzene [22] and alkenes [23]. It has found that the GRO in these nanocomposites has a positive impact in enhancing the catalytic efficiency and selectivity.

The methods for the binding of nanomaterials on the surface of GRO are broadly classified in two different categories i.e., post immobilization (*ex-situ* hybridization) and in situ binding (*in-situ* crystallization). In the post immobilization method, separately prepared dispersions of graphene or graphene oxide and pre-synthesized NPs are mixed to obtain nanocomposite, whereas in-situ binding is performed by the simultaneous reduction of graphene oxide and metal precursors [24]. So far, several methods have been reported for the synthesis of graphene-based nanocomposites, including chemical, electrochemical, microwave based synthesis etc. Among these methods, chemical method is widely used for the large-scale synthesis of graphene-based nanocomposites. However, this method typically involves hazardous chemicals and functionalization ligands, which often have adverse effects on the environment. This gave the impetus to researchers to find alternative eco-friendly methods for the synthesis of graphene based nanocomposites [25]. Recently, the environmental friendly mechanochemical preparation methods have emerged as suitable alternative to the commonly applied chemical approaches for the preparation of nanomaterials with outstanding properties for advanced applications. Nowadays, these methods are also gaining significant popularity for the preparation of graphene-based nanocomposites [26].

Herein, we report the eco-friendly fabrication of Ag₂O–MnO₂/GRO nanocomposites by the solid-state mixing of separately prepared GRO and Ag₂O–MnO₂ NPs using a mechanochemical ball milling method. Notably, the catalytic activity of Ag₂O–MnO₂/GRO nanocomposite has been compared with the HRG based catalyst protocol, i.e. Ag₂O–MnO₂/HRG nanocomposite reported earlier [27]. It has found that the Ag₂O–MnO₂/HRG exhibited lower catalytic performance, which

yielded a 94.1% conversion of BnOH as well as $12.5 \text{ mmol.g}^{-1}.\text{h}^{-1}$ specific performance within 30 minutes at 100°C , whilst $\text{Ag}_2\text{O-MnO}_2/\text{GRO}$ achieved 100% conversion with $13.3 \text{ mmol.g}^{-1}.\text{h}^{-1}$ specific performance under identical reaction conditions. The as-obtained catalysts have been fully characterized using XRD, HR-TEM, SEM, EDX, BET, TGA, FTIR and Raman spectroscopy. Subsequently, to study the catalytic effect of GRO, the as-prepared catalysts were tested towards the aerial oxidation of a variety of alcohols as displayed in Scheme 1. To the best of our knowledge, this is the first study of utilizing $\text{Ag}_2\text{O-MnO}_2/\text{GRO}$ composite as a catalyst for the oxidation of alcohols, highlighting the catalytic efficiency of GRO.



Scheme 1. Fabrication of (1%) $\text{Ag}_2\text{O-MnO}_2/\text{GRO}$ nanocomposite.

2. Results and discussion

2.1. Characterizations

XRD analysis is an imperative technique to study the crystallinity of the synthesized samples. Figure 1 illustrates XRD patterns of the pure graphite, GRO, (1%) $\text{Ag}_2\text{O-MnO}_2$ (without GRO) and (1%) $\text{Ag}_2\text{O-MnO}_2/(5 \text{ wt.}\%)\text{GRO}$ nanocomposite. The XRD spectrum of (1%) $\text{Ag}_2\text{O-MnO}_2$ (Figure 1) contains characteristic diffraction peaks of pyrolusite MnO_2 which are in complete agreement with the published data of (JCPDS file no. 24-0735). On the other hand the (1%) $\text{Ag}_2\text{O-MnO}_2/(5 \text{ wt.}\%)\text{GRO}$ nanocomposite possesses all the diffraction peaks corresponding to the (1%) $\text{Ag}_2\text{O-MnO}_2$ and in addition, it also contains the characteristic (002) peak of GRO at 11.6° (cf. Figure 1, blue line) confirming the formation of nanocomposite.

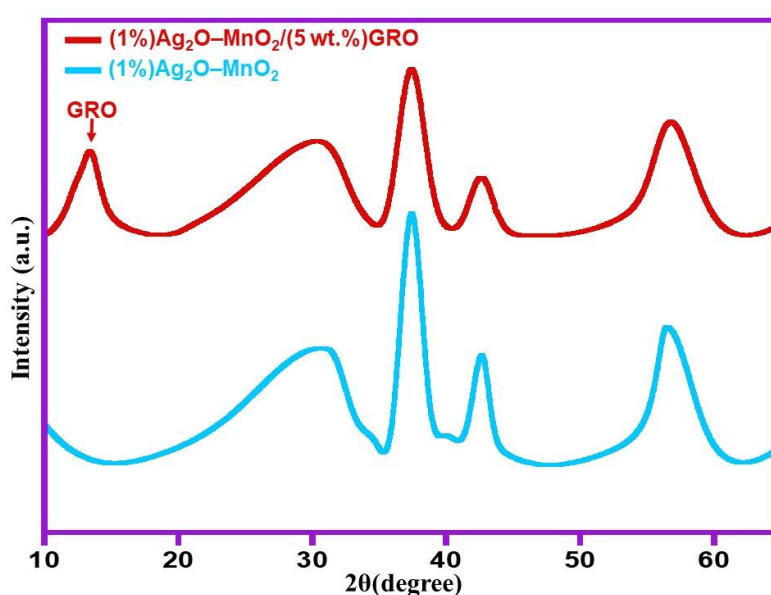


Figure 1. XRD analysis of the (1%) $\text{Ag}_2\text{O-MnO}_2$ and (1%) $\text{Ag}_2\text{O-MnO}_2/(5 \text{ wt.}\%)\text{GRO}$.

The thermal stability of (1%)Ag₂O–MnO₂/(5 wt.%)GRO nanocomposite has been compared with the thermal properties of the precursors (1%)Ag₂O–MnO₂ utilizing TGA, as shown in Figure 2. In comparison, the (1%)Ag₂O–MnO₂/(5 wt.%)GRO composite exhibited a much enhanced thermal stability, which loses only ~18% of its overall weight at 800 °C (cf. Figure 2, purple line), probably owing to the pyrolysis of GRO when exposed to an elevated temperatures [28]. This indicates the high stability of the (1%)Ag₂O–MnO₂/(5 wt.%)GRO composite when compared to (1%)Ag₂O–MnO₂ NPs.

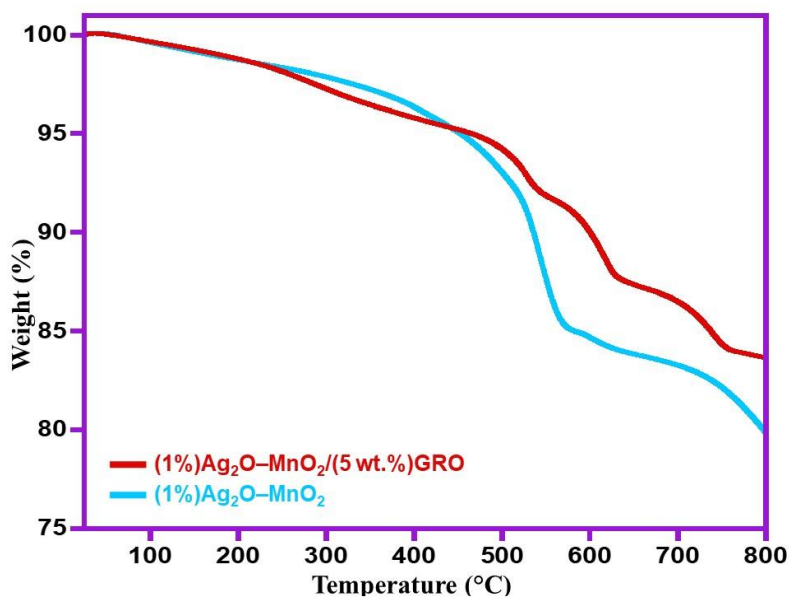


Figure 2. TGA graphs of the (1%)Ag₂O–MnO₂ and (1%)Ag₂O–MnO₂/(5 wt.%)GRO.

Raman analyses are also performed for the samples (1%)Ag₂O–MnO₂ and (1%)Ag₂O–MnO₂/(5 wt.%)GRO as displayed in Figure 3. The Raman spectra of the (1%)Ag₂O–MnO₂ and (1%)Ag₂O–MnO₂/(5 wt.%)GRO nanocomposite exhibited a characteristic peak centered at 642 cm⁻¹. The presence of this peak can be attributed to the symmetric lattice vibration of Mn–O, which point towards the existence of manganese dioxide in both (1%)Ag₂O–MnO₂ and (1%)Ag₂O–MnO₂/(5 wt.%)GRO nanocomposite [29]. Additionally, the Raman spectra of the composite also possess two different characteristic peaks of GRO at 1594 cm⁻¹ and 1340 cm⁻¹ which are assigned to D- and G-band of GRO, respectively [30]. On the other hand the pristine GRO possesses G- and the D-bands at 1604 cm⁻¹ and 1345 cm⁻¹, respectively [31]. Notably, when compared to the pristine GRO, the G-band in nanocomposite is shifted ~10 cm⁻¹ from 1604 cm⁻¹ to 1594 cm⁻¹, while a small shift was detected in the D-band from 1345 cm⁻¹ to 1340 cm⁻¹. These small shifts can be attributed to the interaction between MnO₂ and GRO [32].

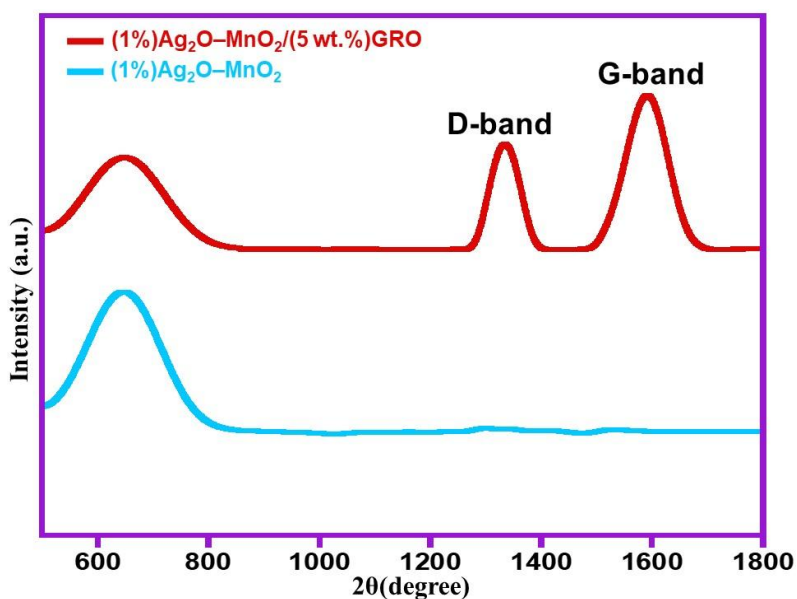


Figure 3. Raman spectra of (1%)Ag₂O–MnO₂ and (1%)Ag₂O–MnO₂/(5 wt.%)GRO.

The morphology and particle size of GRO, (1%)Ag₂O–MnO₂ and (1%)Ag₂O–MnO₂/(5 wt.%)GRO nanocomposite were analyzed by HR-TEM. Figure 4(a) demonstrates highly exfoliated GRO nanolayers, which has a transparent thin flake morphology. Whilst, HR-TEM images of the synthesized (1%)Ag₂O–MnO₂/(5 wt.%)GRO nanocomposite distinctly discloses that the size of the Ag₂O nanoparticles in the catalyst with 0.83 ± 0.12 nm as average size with spherical shape and are well dispersed on the crumpled GRO nanolayers as demonstrated in Figure 4(c,d). Notably, HR-TEM micrograph of the (1%)Ag₂O–MnO₂ without GRO shows the average diameter of Ag₂O NPs in the range of 2.09 ± 0.35 nm, which is larger than the Ag₂O NPs present in the composite, as displayed in Figure 4(b). Presumably, the mechanochemical forces applied during the ball milling process facilitate the formation of the smaller size of NPs in the composite. The presence of smaller size of NPs in the composite as confirmed by the HR-TEM analysis is also reflected by the enhanced surface area and catalytic activity of sample when compare to the (1%)Ag₂O–MnO₂.

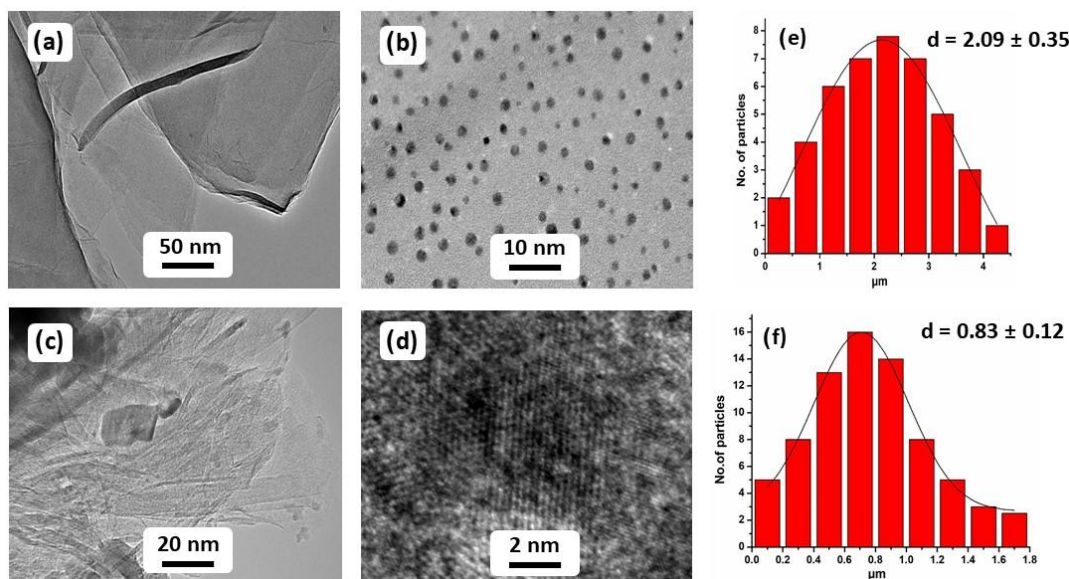


Figure 4. HR-TEM images of (a) GRO, (b) (1%)Ag₂O–MnO₂ catalyst (without GRO), (c,d) (1%)Ag₂O–MnO₂/(5 wt.%)GRO nanocomposite, (e,f) particle size distribution of (1%)Ag₂O–MnO₂ and (1%)Ag₂O–MnO₂/(5 wt.%)GRO nanocomposite, correspondingly.

The morphology of the as-prepared (1%)Ag₂O–MnO₂ and (1%)Ag₂O–MnO₂/(5 wt.%)GRO nanocomposite is also examined by SEM as displayed in Figure 5. The SEM micrographs of the catalyst without GRO i.e. (1%)Ag₂O–MnO₂ showed well-defined cuboidal shaped particles with micro size. Whereas, the nanocomposite displayed much smaller cuboidal shaped microparticles due to ball mill process. The nanoparticles after ball milling causes a smaller but wide size distribution. This will lead to increase the total surface area of the catalyst.

Furthermore, the BET analysis has revealed the surface area of the samples, the surface area of (1%)Ag₂O–MnO₂ (without GRO) is approximately 84 m².g^{−1} as demonstrated in Table 2. Whereas, the nanocomposite after doping with GRO demonstrated an enhanced surface area of 158 m².g^{−1}. These results are in good agreement with the results of SEM and TEM analyses, which revealed the presence of small-sized nanoparticles in the composite. Hence, it is assume that the preparation of (1%)Ag₂O–MnO₂/(5 wt.%)GRO by the induction of GRO through an eco-friendly mechanochemical process leads to the formation of a stable and efficient nanocatalyst.

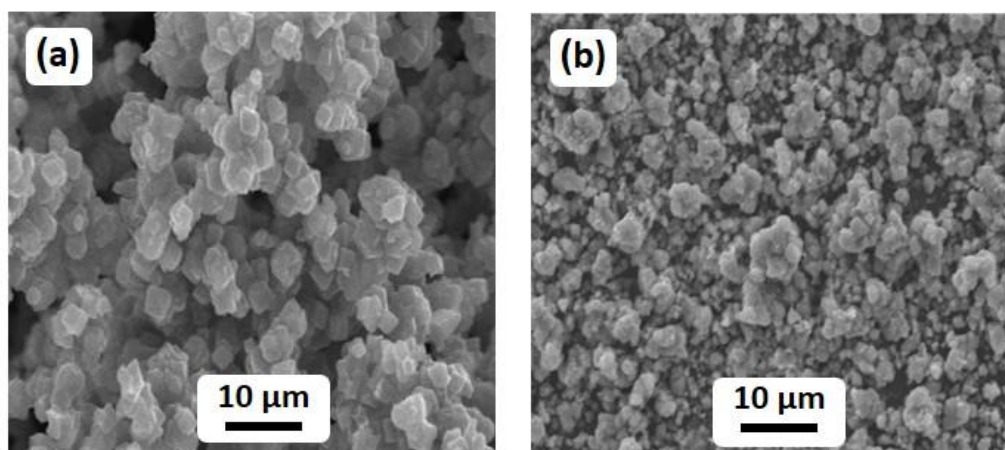


Figure 5. SEM analysis of (a) (1%)Ag₂O–MnO₂ and (b) (1%)Ag₂O–MnO₂ / (5 wt.%)GRO nanocomposite.

2.2. Catalytic Assessment

To assess the catalytic efficacy of the as-prepared nanocomposites, oxidation of BnOH utilizing molecular O₂ as an eco-friendly oxidizing agent was employed as a model substrate. Various catalysts were fabricated by changing the weight percentage of GRO in the nanocomposite. In addition, the influence of catalyst weight, reaction temperature and time on the performance of the prepared catalysts has thoroughly examined to determine the optimum conditions as demonstrated in Figures 6-8 and Tables 1 and 2.

2.2.1. Influence of wt% GRO

The efficacy of the catalytic performance could be enhanced using graphene or its derivatives as a supporting material and an efficient promoter [33][34]. Previously, we have found that the silver oxide nanoparticles was found to be an efficacious promoter to the manganese dioxide, and the (1%)Ag₂O–MnO₂ catalyst annealed at 400 °C exhibited the superior activity for aerial oxidation of alcohols employing gaseous O₂ as a clean oxidizing agent [35]. Therefore, Herein, the (1%)Ag₂O–MnO₂ catalyst has been selected with a target to compare the support effects. However, in order to enhance the catalytic efficiency, the initial studies were done to know the convenient weight percentage of GRO (wt.%) in the synthesized nanocomposite.

First of all, we have tested the performance of pure GRO (300 g) for the aerial oxidation of BnOH with O₂ as an environmentally-friendly oxidant. It has found that the GRO is not active for the BnOH oxidation. However, when the various weight percentages of GRO are introduced to the prepared nanocomposite, i.e. (1%)Ag₂O–MnO₂/(X wt.%)GRO (X = 1 – 7), it is found to have a strong impact on the catalytic efficacy. The obtained results from the catalytic tests were summed up in Table 1.

As seen in Table 1, the catalyst without GRO [(1%)Ag₂O–MnO₂] afforded a 65.0% BnOH conversion within only 30 minutes. However, after doping of the prepared catalyst with 1 and 3 wt.% of GRO, i.e. (1%)Ag₂O–MnO₂/(1 wt.%)GRO and (1%)Ag₂O–MnO₂/(3 wt.%)GRO nanocomposites yielded BnOH conversion of 68.1% and 85.4%, respectively, under the identical circumstances. By further increasing the wt.% of GRO in the nanocomposite i.e. (1%)Ag₂O–MnO₂/(5 wt.%)GRO, the catalytic efficiency remarkably increased and gave a 100% conversion after 30 minutes in addition to 13.3 mmol.g⁻¹.h⁻¹ specific performance. Further increase in the weight percentage of GRO led to slight decline in the effectiveness of the nanocomposite, presumably ascribed to the blocking effect of GRO that can cover the active sites of the catalyst owing to the high wt.% of GRO. Meantime, the BnH selectivity still remains the same during all oxidation processes (<99%). Accordingly, it has deduced that the GRO had a crucial influence in promoting the performance of the current catalytic strategy for this transformation.

Table 1. Oxidation of BnOH using several wt.% of GRO.

Entry	Catalyst	Conv. (%)	Sp. performance (mmol.g ⁻¹ .h ⁻¹)	Sel. (%)
1	GRO	3.2	0.43	<99
2	(1%)Ag ₂ O–MnO ₂	65.0	8.6	<99
3	(1%)Ag ₂ O–MnO ₂ /(1 wt.%)GRO	68.1	9.1	<99
4	(1%)Ag ₂ O–MnO ₂ /(3 wt.%)GRO	85.4	11.3	<99
5	(1%)Ag ₂ O–MnO ₂ /(5 wt.%)GRO	100.0	13.3	<99
6	(1%)Ag ₂ O–MnO ₂ /(7 wt.%)GRO	96.8	12.9	<99

Conditions: 300 mg catalyst, 20 mL.min⁻¹ O₂ rate, 15 mL toluene, 2 mmol BnOH, 100 °C, 30 minutes.

2.2.2. Role of various graphene supports

Based on our former reported publications, we have also compared the efficiency of Ag₂ONPs/MnO₂ immobilized on various graphene supports such as GRO and highly reduced graphene oxide (HRG) for oxidation of BnOH to understand the role of graphene. The obtained data were compiled in Table 2 and depicted in Figure 6. As displayed in Table 2, the undoped catalyst without GRO i.e. (1%)Ag₂O–MnO₂ yielded an 84.3% BnOH conversion of after 30 minutes. This was further raised to 100 % conversion when 5% wt.% of GRO was utilized i.e. (1%)Ag₂O–MnO₂/(5 wt.%)GRO nanocomposite. This catalyst showed remarkably higher catalytic activity giving a full BnOH conversion within only 30 minutes.

Table 2. Catalytic oxidation of BnOH catalyzed by different catalysts.

Entry	Catalyst	Surface area (m ² .g ⁻¹)	Conv. (%)	Sp. performance (mmol.g ⁻¹ .h ⁻¹)	Sel. (%)
1	GRO	85.4	3.2	0.43	<99
2	HRG	78.2	3.0	0.39	<99
3	(1%)Ag ₂ O–MnO ₂	84.3	65.0	8.6	<99
4	(1%)Ag ₂ O–MnO ₂ /(5 wt.%)HRG	149.1	94.1	12.5	<99
5	(1%)Ag ₂ O–MnO ₂ /(5 wt.%)GRO	158.7	100.0	13.3	<99

Conditions: 300 mg catalyst, 15 mL toluene, 20 mL.min⁻¹ O₂ rate, 2 mmol BnOH, 100 °C, 30 minutes.

It is interesting to note that the catalytic activity of HRG based catalyst protocol, i.e. (1%)Ag₂O–MnO₂/(5 wt.%)HRG nanocomposite reported earlier have been compared with the catalytic efficacy of the (1%)Ag₂O–MnO₂/(5 wt.%)GRO nanocomposite [27]. It has found that the (1%)Ag₂O–MnO₂/(5 wt.%)HRG showed lower catalytic efficiency, which afforded a 94.1% conversion of BnOH alongside 12.5 mmol.g⁻¹.h⁻¹ specific performance within 30 minutes at 100 °C, whilst (1%)Ag₂O–MnO₂/(5 wt.%)GRO gave 100% conversion with 13.3 mmol.g⁻¹.h⁻¹ specific performance under similar circumstances. The higher activity of the catalyst using GRO could be due to more homogenous growth of Ag₂ONPs–MnO₂ on the GRO support owing to the existence of superabundant oxygen-carrying groups, which also behaves as nucleation sites. Nevertheless, with respect to HRG, the nucleation sites are less in number that results in more aggregated growth of active catalyst. In addition, the specific surface area of GRO based nanocomposite higher than that of HRG-nanocomposite. Therefore, it can be stated that utilizing GRO for synthesizing the metallic oxide catalysts could be useful for homogeneous growth of catalyst on the surface.

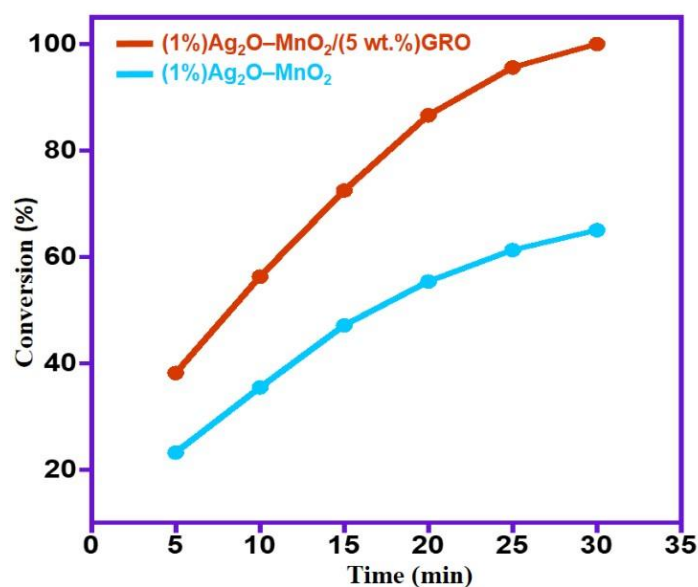


Figure 6. Impact of time on catalytic performances of fabricated catalysts.

2.2.3. Impact of temperature

In general, the temperature played an important role in the catalytic system and had an obvious impact on catalytic efficacy of the catalyst. Therefore, a series of reactions were carried out at different temperatures viz. RT, 40, 60, 80 and 100 °C catalyzed by [(1%)Ag₂O–MnO₂ and (1%)Ag₂O–MnO₂/(5 wt.%)GRO] by maintaining other factors constant. The data presented in the Figure 7 showed that the temperature has positive effect on the effectiveness of all catalysts have employed in the present study. Whilst, the selectivities to BnH were achieved <99% for all catalysts.

Figure 7 shows that the optimum catalyst showed highest activity is the (1%)Ag₂O–MnO₂/(5 wt.%)GRO catalyst. At RT, a lower alcohol conversion of 38.2% was obtained. Unsurprisingly, the elevated reaction temperatures assisted to a higher catalytic efficiency of the catalyst. At 100 °C, a 100% transformation of alcohol was achieved under same catalytic circumstances. Consequently, 100 °C could be considered as the optimum reaction temperature for a higher conversion rate. Hence, it was selected for further studies.

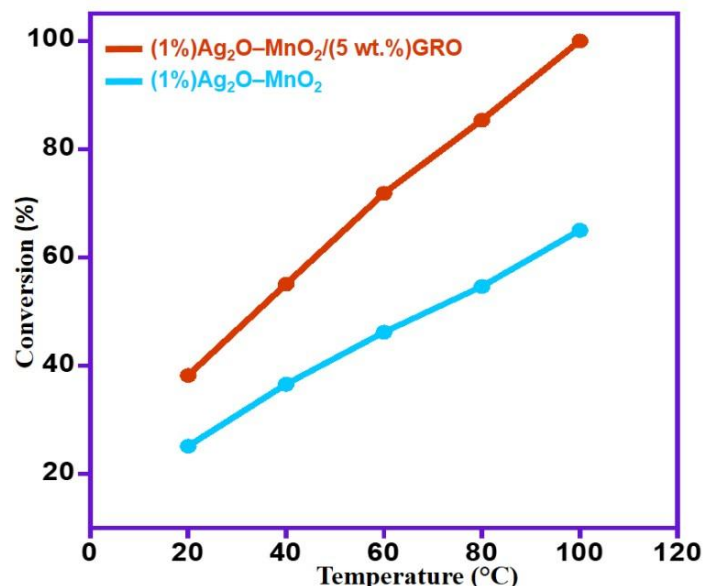


Figure 7. Impact of temperature on the BnOH conversion using various catalysts.

2.2.4. Impact of catalyst dosage

To evaluate the influence of varying amount of catalysts [(1%)Ag₂O-MnO₂ and (1%)Ag₂O-MnO₂/(5 wt.%)GRO], six different quantities (50, 100, 150, 200, 250 and 300 mg) were taken with keeping all other factors constant and the attained catalytic data were plotted in Figure 8. Figure 8 clearly shows that BnOH conversion increased linearly as the catalyst doses raised from 50 mg to 300 mg. However, the selectivity to aldehyde was almost motionless throughout oxidation processes (<99%). Among all catalysts employed in this study, the (1%)Ag₂O-MnO₂/(5 wt.%)GRO catalyst showed superior activity towards BnOH oxidation, when the catalyst amount raised from 50 mg to 300 mg, the conversion of BnOH markedly increased from 29.9% to 100% after 30 minutes. The current study demonstrated that only 300 mg of the catalyst was needed for accomplishing complete conversion of BnOH after short period.

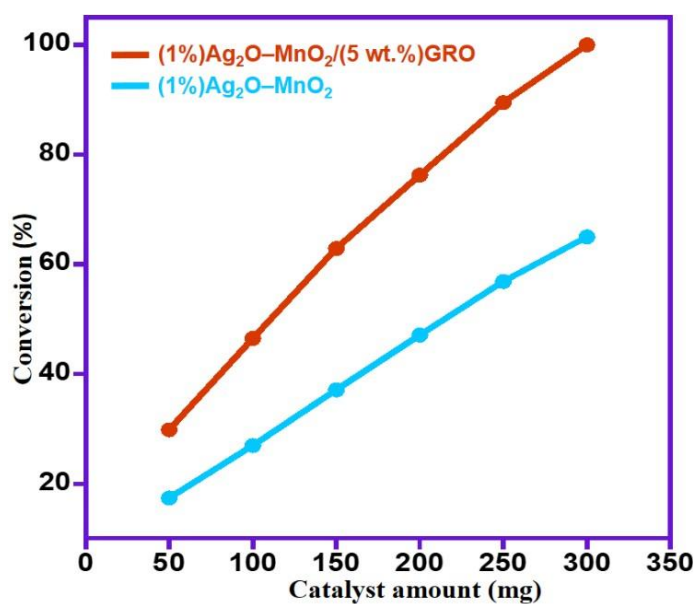


Figure 8. Impact of catalyst quantity on the oxidation of BnOH using various catalysts.

Under the optimum conditions, a blank test (without reactant i.e. BnOH) has been performed using (1%)Ag₂O-MnO₂/(5 wt.%)GRO catalyst in presence of the solvent i.e. toluene to assure that there is no function of solvent in BnOH oxidation. However, no oxidative product (BnH) was detected, implying that the BnH is only produced from the catalytic oxidation of BnOH and not from toluene oxidation. Additionally, a blank test (no catalyst) has also been carried out at the optimized circumstances to ascertain that the produced BnH is being obtained owing to the catalytic efficacy of the fabricated catalyst. It was noticed that no BnH has been noticed, proving that the synthesized catalyst is indispensable for this transformation. Furthermore, to illustrate the importance of the oxidizing agent (O₂), the experiment was performed over (1%)Ag₂O-MnO₂/(5 wt.%)GRO catalyst using air without bubbling O₂. At the optimum circumstances, the obtained data displayed that only 31.8% conversion of BnOH has been detected, which is much lesser than that of 100% convertibility achieved when the process is conducted using gaseous O₂.

2.3. Reusability tests

Recyclability and stability of the catalyst is a significant aspect in enhancement of heterogeneous catalysis systems for the industrial applications. The reusability of the (1%)Ag₂O–MnO₂/(5 wt.%)GRO nanocomposite was investigated for the catalytic oxidation of BnOH at the optimal circumstances. The catalytic activities of the (1%)Ag₂O–MnO₂/(5 wt.%)GRO catalyst at different cycles for BnOH oxidation was illustrated in Figure 9. The reusability data disclosed that we are able to reuse the fabricated catalyst for six runs with no manifest loss in its performance after every cycle. The BnOH conversion decreases slightly from 100% to 90.46% after six recycling experiments, presumably ascribed to the mass loss through the retrieving step [36]. It is interesting to note that BnH selectivity was stayed motionless (<99%) through all recycling reactions. The attained data displayed that our catalyst is resistant to deactivation in aerial oxidation BnOH.

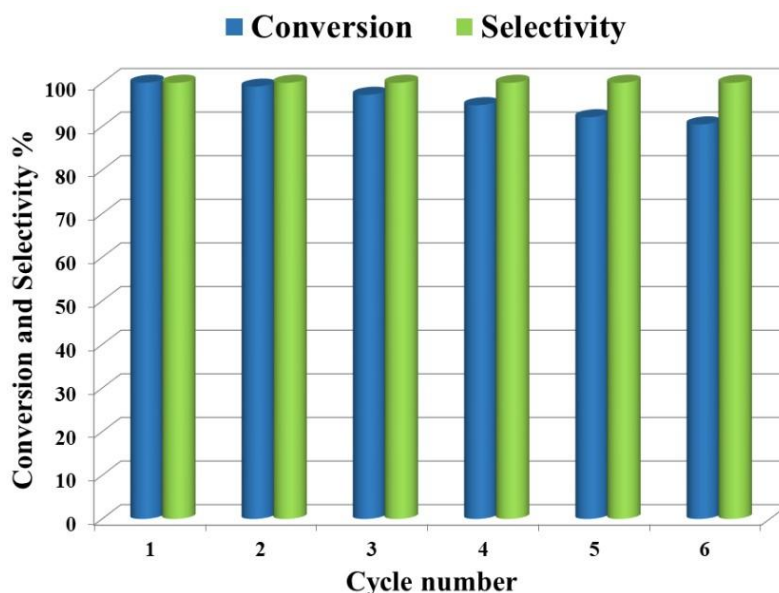


Figure 9. Reusability of (1%)Ag₂O–MnO₂/(5 wt.%)GRO catalyst for BnOH oxidation, Conditions 300 g catalyst, 20 mL.min⁻¹ O₂ rate, 15 mL toluene, 2 mmol BnOH, 100 °C, 30 minutes.

Moreover, to further elucidate the superior efficacy of the (1%)Ag₂O–MnO₂/(5 wt.%)GRO catalyst, this catalyst was compared with formerly recorded graphene containing catalysts as displayed in Table 3. By comparing our catalyst with the other catalysts were compiled in Table 3, (1%)Ag₂O–MnO₂/(5 wt.%)GRO catalyst in this study exhibited higher conversion and specific performance within shorter reaction time. Therefore, it can be said that our catalyst is the most efficient catalyst for BnOH oxidation with regards to higher conversion, selectivity and specific performance, as well as lower reaction time. The (1%)Ag₂O–MnO₂/(5 wt.%)GRO nanocomposite afforded 100% BnOH conversion and <99% selectivity for BnH within 30 minutes alongside outstanding specific performance (13.3 mmol.g⁻¹.h⁻¹). For instance, Rana and his group [37] have fabricated Cu supported amine functionalized graphene oxide (Cu@AGO) and employed for catalytic oxidation of BnOH. The Cu@AGO catalyst gave 92% conversion and BnH selectivity (99%) with specific performance of 2 mmol.g⁻¹.h⁻¹ within 3 h. Feng and his group [38] reported the employ of CuNPs@rGO composite as an effective catalyst for the BnOH oxidation, but it needs a relatively longer reaction time (16 h) to give <99% conversion and 98.6% selectivity towards BnH alongside lower specific performance of 8 mmol.g⁻¹.h⁻¹.

Table 3. Comparison of various graphene catalysts for selective oxidation of BnOH.

Catalyst	Conv. (%)	Sel. (%)	Time	T. (°C)	Sp. performance (mmol.g ⁻¹ .h ⁻¹)	Ref.
Ag ₂ O–MnO ₂ /(5 wt.%)GRO	100	>99	30 min	100	13.3	This work
Ag ₂ O–MnO ₂ /(5 wt.%)HRG	94.1	>99	30 min	100	12.5	[27]
Cu@AGO	92	99	3 h	70	2.1	[37]
CuNPs@rGO	>99	98.6	16 h	80	8.3	[38]
AgNPs/GRO	33	55	24 h	80	2.8	[39]
AgNPs/rGO	12	8	24 h	80	1.0	[39]
Im-PW/GRO	90.8	99.2	7 h	90	8.6	[40]
Au/RGO	65	93	8 h	100	5.4	[36]

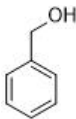
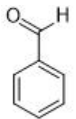
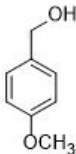
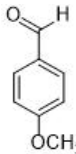
Pd NPs/GRO	36	34.1	6 h	110	1.0	[34]
1%RGO–MnCoO	78	100	2 h	140	12.6	[41]
GRO–N–PW	76	99	6 h	100	10.6	[42]
MnO ₂ /GRO	97	100	3 h	110	1.6	[33]
Pd(II)-AAPTMS@GRO	96	99	3 h	60	2.1	[43]

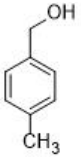
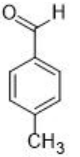
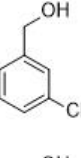
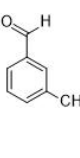
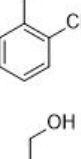
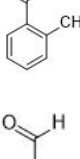
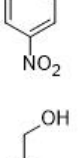
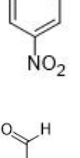
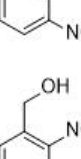
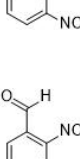
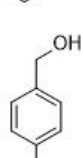
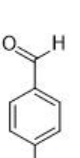
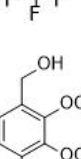
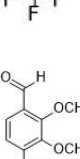
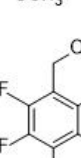
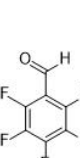
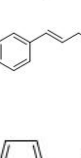
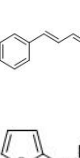
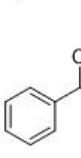
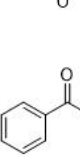
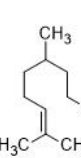
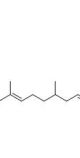
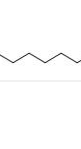
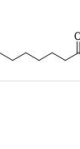
2.4. General applicability

Moreover, Ag₂O–MnO₂/(5 wt.%)GRO has found to be an efficient and selective for the aerial oxidation of various kinds of alcohols, an indication of its considerable versatility. According to Table 4, all primary benzylic alcohols were easily oxidized to their respective aldehyde derivatives with 100% conversions within relatively short periods (Table 4, entries 1–11). Besides, perfect selectivities (<99%) toward respective aldehydes were accomplished for all alcohols that used in this study without further oxidation to carboxylic acids. It can be observed that the nature of substituents (electron-releasing or electron-withdrawing) on the benzylic alcohols has an explicit impact on the oxidation rate. Benzylic alcohols bearing electron-releasing groups were found to be more active and were oxidized to the respective aldehydes in shorter reaction periods. The rate of oxidation process was slower when the benzyl alcohol contained an electron-withdrawing group. That might ascribed to the decrease of electronic cloud density on aromatic ring caused by -ve induction effect [44]. Additionally, it was observed that the *p*-substituted benzyl alcohols is easily oxidized by comparing with the *ortho*- and *meta*-substituted alcohols, presumably due to the *para*-derivative has lower steric hindrance by comparing with other derivatives [30]. In this regard, *p*-methylbenzyl alcohol was wholly converted to *p*-methylbenzaldehyde within only 35 minutes (Table 4, entry 3), whereas *o*- and *m*-methylbenzyl alcohol were fully oxidized within longer times of 45 and 50 minutes, correspondingly (Table 4, entries 4 and 5). It was also found that the steric hindrance had a significant effect on the oxidation rate, the bulk group (e.g., trifluoromethyl, trimethoxy and pentafluoro) connected to benzyl alcohol reduce the efficiency of the oxidation process, might be owing to the steric hindrance that prohibits oxidation of the alcohols possessing bulk groups (Table 4, entries 9–11) [45]. It is noteworthy to mention that cinnamyl alcohol as an example of allylic alcohol achieved 100% conversion and <99% selectivity of cinnamaldehyde within 50 minutes (Table 4, entry 12). Regarding furfuryl alcohol as an example of hetero-aromatic alcohol has also wholly transformed to furfural after 110 minutes (Table 4, entry 13). Moreover, the current catalytic methodology has also applicable to the oxidation of secondary benzylic alcohols, for example, α -phenyl-ethanol was selectively transformed to acetophenone with complete conversion within only 25 min (Table 4, entry 14)

Indeed, the oxygenation of aliphatic alcohols is significantly more complicated with respect to the aromatic counterparts [46], excellent results are obtained by oxidation of primary aliphatic alcohols using the present catalytic strategy. In this regard, the oxidation of citronellol into the citronellal occurs in relatively longer reaction times (Table 4, entries 15). Compared to secondary benzylic alcohols, the oxidation of secondary aliphatic alcohols showed a lower reactivity towards this oxidation transformation. Obviously, it was indispensable to elongate the time, due to the oxidation of benzylic secondary alcohols is easier than that of aliphatic ones. As estimated, full oxidation of α -phenyl-ethanol occurs within only 25 minutes, while the entire oxidation of 2-octanol occurred after longer time of 240 minutes (Table 4, entries 14 and 16). Accordingly, the present catalytic methodology has affected by dual factors, electronic and steric impacts. As a conclusion, in general, the current catalytic oxidation protocol has found to be efficacious for oxygenation of various kinds of alcohols include benzylic, aliphatic, allylic, heterocyclic, primary and secondary alcohols, indicating the versatility of Ag₂O–MnO₂/(5 wt.%)GRO catalyst for aerial selective alcohol oxidation.

Table 4. Aerial oxidation of several kinds of alcohols using Ag₂O–MnO₂/(5 wt.%)GRO with O₂ under alkali free conditions.

Entry	Substrate	Product	time (min)	Conv. (%) / Sel. (%)
1			30	100/>99
2			30	100/>99

3			35	100/>99
4			45	100/>99
5			50	100/>99
6			55	100/>99
7			60	100/>99
8			70	100/>99
9			60	100/>99
10			60	100/>99
11			75	100/>99
12			50	100/>99
13			110	100/>99
14			25	100/>99
15			120	100/>99
16			240	100/>99

Conditions: 2 mmol alcohol, 15 mL toluene, 300 mg Ag₂O–MnO₂/(5 wt.%)GRO catalyst, 20 mL.min⁻¹ O₂ rate and 100 °C.

3. Experimental

3.1. Synthesis of GRO

Initially, GRO was fabricated from pristine graphite through the Hummer's method ^[47].

3.2. Synthesis of Ag₂O–MnO₂ Nanoparticles

The Ag₂O–MnO₂ was prepared separately through a co-precipitation procedure. In brief, stoichiometric amounts of AgNO₃ and Mn(NO₃)₂ were dissolved in distilled water (100 ml) followed by the dropwise addition of 0.5 M NaHCO₃ solution at 100 °C for 3 hrs (till the pH of the resultant solution reaches to 9). A vigorous stirring of the resultant mixture was continued over-night at RT. The reaction mixture was filtered via centrifugation and dried at 70 °C for 12 hrs. The as-obtained nanomaterial was annealed at 300 °C for 24 hrs and further used for the preparation of nanocomposite. Subsequently, the previously prepared GRO dried at 70 °C, is introduced in the Ag₂O–MnO₂ by milling to synthesize the desired (1%)Ag₂O–MnO₂/GRO catalyst. It is important to note that if GRO was incorporated before the calcination process, there was a significant decrease in weight and catalytic activity.

3.3. Synthesis of Ag₂O–MnO₂/GRO nanocomposite

For this purpose, the GRO was prepared using a previously reported modified Hummer's method using natural graphite and dried overnight at 40 °C. Approximately 1.90 g of Ag₂O–MnO₂ nanoparticles and 0.1 g of GRO powder were milled using Fritsch Pulverisette P7 planetary ball mill. The Graphite Oxide Powder and Stainless Steel balls (5 mm Diameter) with a ball to powder weight ratio of 11:1 were introduced into the Stainless Steel Container. The milling of the powder was performed for 16 hours. And in order to maintain the temperature inside the container, the milling process was paused at regular intervals).

3.4. Catalyst Characterization

The prepared materials were characterized using several instruments and all experimental details are described in the supplementary file.

3.5. Catalytic Assessment

Oxidation of benzyl alcohol was performed in a glass flask equipped with a magnetic stirrer, reflux condenser, and thermometer. A mixture of benzyl alcohol (2 mmol), toluene (10 mL), and the catalyst (0.3 g) was transferred in a glass three-necked round-bottomed flask; the resulting mixture was then heated to the desired temperature with vigorous stirring. The oxidation experiment was started by bubbling O₂ gas at a flow rate of 20 mL.min⁻¹ into the reaction mixture. After the reaction, the solid catalyst was filtered off by centrifugation and the liquid products were analyzed by gas chromatography to determine the conversion of the alcohol and product selectivity by (GC, 7890A) Agilent Technologies Inc, equipped with a flame ionization detector (FID) and a 19019S-001 HP-PONA column.

3.6. Reusability tests

After the completion of first oxidation process, the used catalyst was separated by centrifuge, then washed many times with toluene and dried at 95 °C for 5 hrs for the next run. The dried catalyst was used for next run under similar aforementioned conditions.

4. Conclusions

Herein we report a cost-effective and eco-friendly mechanochemical approach for the preparation of GRO based Ag₂O–MnO₂ nanocatalyst for the aerial oxidation of a variety of alcohols. The nanocatalyst has demonstrated a high conversion ability (~100%)and excellent selectivity in the presence of O₂ as clean oxidant without utilizing any hazardous surfactants or bases. Under the optimum conditions, (1%)Ag₂O–MnO₂/(5 wt.%)GRO catalyst exhibited better catalytic performance (100% conversion) in comparison with Ag₂O–MnO₂ catalyst. The higher catalytic properties of the nanocomposite is attributed to the presence of GRO which exhibits extraordinary catalytic properties like high surface area, excellent chemical compatibility and stability, superior mechanical and thermal stability as well as the presence of several defects. The eco-friendly, physical blending of the components including GRO and Ag₂O–MnO₂ NPs at RT avoided the pyrolysis of

oxygen containing functional groups, which allows to preserve the defects and active sites of the resulting composite. Therefore, (1%)Ag₂O–MnO₂/(5 wt.%)GRO showed a 100% conversion of BnOH with ~99% selectivity towards the formation of BnH within a relatively short time. The obtained specific performance (13.3 mmol.g⁻¹.h⁻¹) was much better than that presented in previous literature. Our catalytic strategy is highly selective, producing only desired products with no over-oxygenation to carboxylic acids. The merits of our catalytic methodology are: (a) facile process, (b) inexpensive and clean oxidant, (c) no surfactants or nitrogenous bases are required, (d) mild catalytic conditions, (e) cost-effective recoverable catalyst, (f) complete convertibility, (g) full selectivity, (h) rapid process and (i) applicable to virtually all types of alcohols. So, these highlights make this catalytic strategy to be highly applicable in the industrial applications for manufacturing of carbonyls.

References

1. Ekaterina Kolobova; Y. Kotolevich; Ekaterina Pakrieva; G. Mamontov; M.H. Farias; Vicente Cortés Corberán; N. Bogdanichikova; J. Hemming; A. Smeds; P. Mäki-Arvela; et al. Modified Ag/TiO₂ systems: Promising catalysts for liquid-phase oxidation of alcohols. *Fuel* **2018**, 234, 110-119, [10.1016/j.fuel.2018.06.128](#).
2. Alaa J. Faqeeh; Tarek T. Ali; Sulaiman N. Basahel; Katabathini Narasimharao; Nanosized samarium modified Au-Ce 0.5 Zr 0.5 O 2 catalysts for oxidation of benzyl alcohol. *Molecular Catalysis* **2018**, 456, 10-21, [10.1016/j.mcat.2018.06.021](#).
3. Kun Liu; Tao Qin; Yongbin Sun; Chao Hou; Xiao-Qun Cao; Shoujun Jiang; Synergistic effect between Ag and Mn 3 O 4 in the gas phase oxidation of alcohols. *Catalysis Communications* **2018**, 113, 15-18, [10.1016/j.catcom.2018.05.002](#).
4. Xinyan Dai; Kowsalya Devi Rasamani; Siyu Wu; Yugang Sun; Enabling selective aerobic oxidation of alcohols to aldehydes by hot electrons in quantum-sized Rh nanocubes. *Materials Today Energy* **2018**, 10, 15-22, [10.1016/j.mtener.2018.08.003](#).
5. Serena Biella; Michele Rossi; Gas phase oxidation of alcohols to aldehydes or ketones catalysed by supported gold.. *Chemical Communications* **2003**, 3, 378-379, [10.1039/b210506c](#).
6. Mujeeb Khan; Muhammad Nawaz Tahir; Syed Farooq Adil; Hadayat Ullah Khan; Mohammed Rafiq H. Siddiqui; Mufsir Kuniyil; Wolfgang Tremel; Graphene based metal and metal oxide nanocomposites: synthesis, properties and their applications. *Journal of Materials Chemistry A* **2015**, 3, 18753-18808, [10.1039/c5ta02240a](#).
7. Kian Ping Loh; Qiaoliang Bao; Priscilla Kailian Ang; JiaXiang Yang; The chemistry of graphene. *Journal of Materials Chemistry* **2010**, 20, 2277, [10.1039/b920539j](#).
8. Xiaobin Fan; Guoliang Zhang; Multiple roles of graphene in heterogeneous catalysis. *Chemical Society Reviews* **2015**, 44, 3023-3035, [10.1039/C5CS00094G](#).
9. Chenliang Su; Kian Ping Loh; Carbocatalysts: Graphene Oxide and Its Derivatives. *Accounts of Chemical Research* **2012**, 46, 2275-2285, [10.1021/ar300118v](#).
10. Chenliang Su; Muge Acik; Kazuyuki Takai; Jiong Lu; Si-Jia Hao; Y. Zheng; Pingping Wu; Qiaoliang Bao; Toshiaki Enoki; Yves J. Chabal; et al. Probing the catalytic activity of porous graphene oxide and the origin of this behaviour. *Nature Communications* **2012**, 3, 1298, [10.1038/ncomms2315](#).
11. Asma A. Ali; Metwally Madkour; Fakhreia Al Sagheer; Mohamed I. Zaki; Ahmed Abdel-Nazeer; Low-Temperature Catalytic CO Oxidation Over Non-Noble, Efficient Chromia in Reduced Graphene Oxide and Graphene Oxide Nanocomposites. *Catalysts* **2020**, 10, 105, [10.3390/catal10010105](#).
12. Mayakrishnan Gopiraman; Somasundaram Saravanamoorthy; Dian Deng; Andivelu Ilangovan; Ick Soo Kim; Ill Min Chung; Facile Mechanochemical Synthesis of Nickel/Graphene Oxide Nanocomposites with Unique and Tunable Morphology: Applications in Heterogeneous Catalysis and Supercapacitors. *Catalysts* **2019**, 9, 486, [10.3390/catal9050486](#).
13. Weining Sun; Xiaofeng Lu; Yan Tong; Zhen Zhang; Junyu Lei; Guang-Di Nie; Ce Wang; Fabrication of highly dispersed palladium/graphene oxide nanocomposites and their catalytic properties for efficient hydrogenation of p-nitrophenol and hydrogen generation. *International Journal of Hydrogen Energy* **2014**, 39, 9080-9086, [10.1016/j.ijhydene.2014.03.197](#).
14. Lidong Shao; Xing Huang; Detre Teschner; Wei Zhang; Gold Supported on Graphene Oxide: An Active and Selective Catalyst for Phenylacetylene Hydrogenations at Low Temperatures. *ACS Catalysis* **2014**, 4, 2369-2373, [10.1021/cs5002724](#).
15. Chao Xu; Xin Wang; Junwu Zhu; Xuejie Yang; Lude Lu; Deposition of Co₃O₄ nanoparticles onto exfoliated graphite oxide sheets. *Journal of Materials Chemistry* **2008**, 18, 5625, [10.1039/b809712g](#).
16. Syed F. Adil; Mohamed E. Assal; Mohammed Rafi Shaik; Mufsir Kuniyil; Nawaf M. Alotaibi; Mujeeb Khan; Muhammad Sharif; M. Mujahid Alam; Mufsir Kuniyil; Jabair A. Mohammed; et al. A Facile Synthesis of ZrO_x-MnCO₃/Graphene Oxide

e (GRO) Nanocomposites for the Oxidation of Alcohols using Molecular Oxygen under Base Free Conditions. *Catalysts* **2019**, 9, 759, [10.3390/catal9090759](https://doi.org/10.3390/catal9090759).

17. Yuyang Liu; Wei Jin; Yaping Zhao; Guangshan Zhang; Wen Zhang; Enhanced catalytic degradation of methylene blue by α -Fe₂O₃/graphene oxide via heterogeneous photo-Fenton reactions. *Applied Catalysis B: Environmental* **2017**, 206, 642-652, [10.1016/j.apcatb.2017.01.075](https://doi.org/10.1016/j.apcatb.2017.01.075).
18. Mohamed E. Assal; Mohammed Rafi Shaik; Mufsir Kuniyil; Mujeeb Khan; Abdulrahman Al-Warthan; Mohammed Rafiq H. Siddiqui; Sohail M. A. Khan; Wolfgang Tremel; Muhammad Nawaz Tahir; Syed Farooq Adil; et al. A highly reduced graphene oxide/ZrO₂–MnCO₃ or –Mn₂O₃ nanocomposite as an efficient catalyst for selective aerial oxidation of benzylic alcohols. *RSC Advances* **2017**, 7, 55336-55349, [10.1039/C7RA11569E](https://doi.org/10.1039/C7RA11569E).
19. Selvamani Arumugam; Babu Cadiam Mohan; Srinivasan Vinju Vasudevan; Ramkumar Vanaraj; Balasubramanian Rukmanikrishnan; Thirukumaran Periyasamy; Shakila Parveen Asrafali; Selective Oxidation of Cyclohexane Using Graphene Oxide-Supported Ceria Nanocomposites with Exposed Active {1 0 0} Facets. *ChemistrySelect* **2017**, 2, 6223-6230, [10.1002/slct.201700769](https://doi.org/10.1002/slct.201700769).
20. Binhua Zhao; Jinyin Liu; Litao Zhou; Dan Long; Kun Feng; Xuhui Sun; Jun Zhong; Probing the electronic structure of M-graphene oxide (M = Ni, Co, NiCo) catalysts for hydrolytic dehydrogenation of ammonia borane. *Applied Surface Science* **2016**, 362, 79-85, [10.1016/j.apsusc.2015.11.205](https://doi.org/10.1016/j.apsusc.2015.11.205).
21. Cheng Wang; Liya Hu; Yichen Hu; Yuanhang Ren; Xueying Chen; Bin Yue; Heyong He; Direct hydroxylation of benzene to phenol over metal oxide supported graphene oxide catalysts. *Catalysis Communications* **2015**, 68, 1-5, [10.1016/j.catcom.2015.04.014](https://doi.org/10.1016/j.catcom.2015.04.014).
22. Jiangyong Diao; Hongyang Liu; Jia Wang; Zhenbao Feng; Tong Chen; Changxi Miao; Weimin Yang; Dang Sheng Su; Porous graphene-based material as an efficient metal free catalyst for the oxidative dehydrogenation of ethylbenzene to styrene. *Chemical Communications* **2015**, 51, 3423-3425, [10.1039/C4CC08683J](https://doi.org/10.1039/C4CC08683J).
23. Qingshan Zhao; Chan Bai; Wenfeng Zhang; Yang Li; Guoliang Zhang; Fengbao Zhang; Xiaobin Fan; Catalytic Epoxidation of Olefins with Graphene Oxide Supported Copper (Salen) Complex. *Industrial & Engineering Chemistry Research* **2014**, 53, 4232-4238, [10.1021/ie500017z](https://doi.org/10.1021/ie500017z).
24. Abdulhadi H. Al-Marri; Merajuddin Khan; Mohammed Rafi Shaik; Nils Mohri; Syed Farooq Adil; Mufsir Kuniyil; Hamad Z. Alkathlan; Abdulrahman Al-Warthan; Wolfgang Tremel; Muhammad Nawaz Tahir; et al. Green synthesis of Pd@graphene nanocomposite: Catalyst for the selective oxidation of alcohols. *Arabian Journal of Chemistry* **2016**, 9, 835-845, [10.1016/j.arabjc.2015.12.007](https://doi.org/10.1016/j.arabjc.2015.12.007).
25. Abdulhadi H. Al-Marri; Mujeeb Khan; Merajuddin Khan; Syed F. Adil; Mufsir Kuniyil; Hamad Z. Alkathlan; Wolfgang Tremel; Joselito Puzon Labis; Mohammed Rafiq H. Siddiqui; Muhammad Nawaz Tahir; et al. Pulicaria glutinosa Extract: A Toolbox to Synthesize Highly Reduced Graphene Oxide-Silver Nanocomposites. *International Journal of Molecular Sciences* **2015**, 16, 1131-1142, [10.3390/ijms16011131](https://doi.org/10.3390/ijms16011131).
26. Esther Rincon; Araceli García; Antonio Angel Romero; Luis Serrano Cantador; Rafael Luque; Alina M. Balu; Mechanochemical Preparation of Novel Polysaccharide-Supported Nb₂O₅ Catalysts. *Catalysts* **2019**, 9, 38, [10.3390/catal9010038](https://doi.org/10.3390/catal9010038).
27. Mohamed E. Assal; Mohammed Rafi Shaik; Mufsir Kuniyil; Mujeeb Khan; Abdulrahman Al-Warthan; Abdulrahman Ibrahim Alharthi; Ravi Varala; Mohammed Rafiq H. Siddiqui; Syed Farooq Adil; Ag₂O nanoparticles/MnCO₃–Mn₂O₃/highly reduced graphene oxide composites as an efficient and recyclable oxidation catalyst. *Arabian Journal of Chemistry* **2019**, 12, 54-68, [10.1016/j.arabjc.2018.03.021](https://doi.org/10.1016/j.arabjc.2018.03.021).
28. Onder Metin; Emine Kayhan; Saim Ozkar; Jörg J. Schneider; Palladium nanoparticles supported on chemically derived graphene: An efficient and reusable catalyst for the dehydrogenation of ammonia borane. *International Journal of Hydrogen Energy* **2012**, 37, 8161-8169, [10.1016/j.ijhydene.2012.02.128](https://doi.org/10.1016/j.ijhydene.2012.02.128).
29. Guangqiang Han; Yun Liu; Erjun Kan; Jian Tang; Lingling Zhang; Huanhuan Wang; Weihua Tang; Sandwich-structured MnO₂/polypyrrole/reduced graphene oxide hybrid composites for high-performance supercapacitors. *RSC Advances* **2014**, 4, 9898-9904, [10.1039/c3ra47764a](https://doi.org/10.1039/c3ra47764a).
30. Mona Hosseini-Sarvari; Tahereh Ataee-Kachouei; Fatemeh Moeini; A novel and active catalyst Ag/ZnO for oxidant-free dehydrogenation of alcohols. *Materials Research Bulletin* **2015**, 72, 98-105, [10.1016/j.materresbull.2015.07.019](https://doi.org/10.1016/j.materresbull.2015.07.019).
31. Shi Liu; Jun Yan; Guangwu He; Dandan Zhong; Jiaxing Chen; Liying Shi; Xuemin Zhou; Jian Shen; Layer-by-layer assembled multilayer films of reduced graphene oxide/gold nanoparticles for the electrochemical detection of dopamine. *Journal of Electroanalytical Chemistry* **2012**, 672, 40-44, [10.1016/j.jelechem.2012.03.007](https://doi.org/10.1016/j.jelechem.2012.03.007).
32. Dhanushkotti Rajesh; Chinnathambi Mahendiran; Chinnathambi Suresh; Arumugam Pandurangan; T. Maiyalagan; Hydrothermal synthesis of three dimensional reduced graphene oxide-multiwalled carbon nanotube hybrids anchored with p

alladium-cerium oxide nanoparticles for alcohol oxidation reaction. *International Journal of Hydrogen Energy* **2019**, *44*, 4962-4973, [10.1016/j.ijhydene.2019.01.025](https://doi.org/10.1016/j.ijhydene.2019.01.025).

33. Zonggao Hu; Yafei Zhao; Jindun Liu; Jingtao Wang; Bing Zhang; Xu Xiang; Ultrafine MnO₂ nanoparticles decorated on graphene oxide as a highly efficient and recyclable catalyst for aerobic oxidation of benzyl alcohol. *Journal of Colloid and Interface Science* **2016**, *483*, 26-33, [10.1016/j.jcis.2016.08.010](https://doi.org/10.1016/j.jcis.2016.08.010).
34. Guangjun Wu; Xueming Wang; Naijia Guan; Landong Li; Palladium on graphene as efficient catalyst for solvent-free aerobic oxidation of aromatic alcohols: Role of graphene support. *Applied Catalysis B: Environmental* **2013**, *136*, 177-185, [10.1016/j.apcatb.2013.01.067](https://doi.org/10.1016/j.apcatb.2013.01.067).
35. Mohamed E. Assal; Mohammed Rafi Shaik; Mufsir Kuniyil; Mujeeb Khan; J. V. Shanmukha Kumar; Abdulrahman Yahya Alzahrani; Abdulrahman Al-Warthan; Saad Abdulaziz Al-Tamrah; Mohammed Rafiq H. Siddiqui; Syed Azhar Hashmi; et al. Silver-doped manganese based nanocomposites for aerial oxidation of alcohols. *Materials Express* **2018**, *8*, 35-54, [10.1166/mex.2018.1409](https://doi.org/10.1166/mex.2018.1409).
36. Xianqin Yu; Yujia Huo; Jing Yang; Sujie Chang; Yunsheng Ma; Weixin Huang; Reduced graphene oxide supported Au nanoparticles as an efficient catalyst for aerobic oxidation of benzyl alcohol. *Applied Surface Science* **2013**, *280*, 450-455, [10.1016/j.apsusc.2013.05.008](https://doi.org/10.1016/j.apsusc.2013.05.008).
37. Surjakanta Rana; Sreekantha B. Jonnalagadda; Cu doped amine functionalized graphene oxide and its scope as catalyst for selective oxidation. *Catalysis Communications* **2017**, *100*, 183-186, [10.1016/j.catcom.2017.07.002](https://doi.org/10.1016/j.catcom.2017.07.002).
38. Xue Feng; Panpan Lv; Wei Sun; Xinyu Han; Lingfeng Gao; Gengxiu Zheng; Reduced graphene oxide-supported Cu nanoparticles for the selective oxidation of benzyl alcohol to aldehyde with molecular oxygen. *Catalysis Communications* **2017**, *99*, 105-109, [10.1016/j.catcom.2017.05.013](https://doi.org/10.1016/j.catcom.2017.05.013).
39. Bahareh Zahed; Hassan Hosseini-Monfared; A comparative study of silver-graphene oxide nanocomposites as a recyclable catalyst for the aerobic oxidation of benzyl alcohol: Support effect. *Applied Surface Science* **2015**, *328*, 536-547, [10.1016/j.apsusc.2014.12.078](https://doi.org/10.1016/j.apsusc.2014.12.078).
40. Wei-Hong Zhang; Jia-Jia Shen; Jing Wu; Xue-Yuan Liang; Jie Xu; Ping Liu; Bing Xue; Yong-Xin Li; An amphiphilic graphene oxide-immobilized polyoxometalate-based ionic liquid: A highly efficient triphase transfer catalyst for the selective oxidation of alcohols with aqueous H₂O₂. *Molecular Catalysis* **2017**, *443*, 262-269, [10.1016/j.mcat.2017.10.018](https://doi.org/10.1016/j.mcat.2017.10.018).
41. Ajay Jha; Dattakumar Mhamane; Anil Suryawanshi; Sameer M. Joshi; Parvez Shaikh; Narayan Biradar; Satish Chandra Ogale; Chandrashekhar V. Rode; Triple nanocomposites of CoMn₂O₄, Co₃O₄ and reduced graphene oxide for oxidation of aromatic alcohols. *Catalysis Science & Technology* **2014**, *4*, 1771, [10.1039/c3cy01025b](https://doi.org/10.1039/c3cy01025b).
42. Kun Liu; Tingting Chen; Zhiqiang Hou; Yuanyuan Wang; Liyi Dai; Graphene Oxide as Support for the Immobilization of Phosphotungstic Acid: Application in the Selective Oxidation of Benzyl Alcohol. *Catalysis Letters* **2013**, *144*, 314-319, [10.1007/s10562-013-1121-4](https://doi.org/10.1007/s10562-013-1121-4).
43. Surjakanta Rana; Suresh Maddila; Sreekantha B. Jonnalagadda; Synthesis and characterization of Pd(II) dispersed over diamine functionalized graphene oxide and its scope as a catalyst for selective oxidation. *Catalysis Science & Technology* **2015**, *5*, 3235-3241, [10.1039/C5CY00192G](https://doi.org/10.1039/C5CY00192G).
44. Cai Xu; Lingling Zhang; Yu An; Xiaozhong Wang; Gang Xu; Yingqi Chen; Liyan Dai; Promotional synergistic effect of Sn doping into a novel bimetallic Sn-W oxides/graphene catalyst for selective oxidation of alcohols using aqueous H₂O₂ without additives. *Applied Catalysis A: General* **2018**, *558*, 26-33, [10.1016/j.apcata.2018.03.017](https://doi.org/10.1016/j.apcata.2018.03.017).
45. Rosmita Borthakur; Mrityunjaya Asthana; Arvind Kumar; Ram A. Lal; Cooperative catalysis by polymetallic copper-zinc complexes in the efficient oxidation of alcohols under solvent free condition. *Inorganic Chemistry Communications* **2014**, *46*, 198-201, [10.1016/j.inoche.2014.05.018](https://doi.org/10.1016/j.inoche.2014.05.018).
46. Elham Assady; Bahram Yadollahi; Mostafa Riahi Farsani; Majid Moghadam; Zinc polyoxometalate on activated carbon: an efficient catalyst for selective oxidation of alcohols with hydrogen peroxide. *Applied Organometallic Chemistry* **2015**, *29*, 561-565, [10.1002/aoc.3332](https://doi.org/10.1002/aoc.3332).
47. William S. Hummers; Richard E. Offeman; Preparation of Graphitic Oxide. *Journal of the American Chemical Society* **1958**, *80*, 1339-1339, [10.1021/ja01539a017](https://doi.org/10.1021/ja01539a017).